Initial Assessment of BDS Zone Correction

Yize Zhang, Junping Chen, Sainan Yang and Qian Chen

Abstract Zone correction is a new type of differential corrections for BeiDou wide area augmentation system. As broadcasted together with the equivalent satellite clock and orbit corrections by BDS satellites, they enable user decimeter-level real-time positioning capability using the carrier-phase observations. In this paper, we give a brief introduction of zone corrections, and the function model of precise point positioning (PPP) for dual- and single-frequency users using the zone corrections. Tracking data of 30 stations in mainland China are used to evaluate the zone-divided PPP performance, and the handling of troposphere delay and ionosphere delay are discussed. Results show that the zone-divided PPP performance improves when fixing the troposphere delay. Model of UofC is much suitable for single frequency user. The dual-frequency PPP can convergences to 0.5 m in 25 min and the positioning accuracy are 0.15 m in horizontal and 0.2 m in vertical, respectively. As for single frequency PPP, the positioning accuracy convergences to 0.8 m in 20 min, while the positioning accuracy is 0.3 m in horizontal and 0.5 m in vertical.

Keywords BDS · Zone correction · Equivalent satellite clock · Convergence time · Precise point positioning

Y. Zhang · J. Chen (✉) · S. Yang · Q. Chen
Shanghai Astronomical Observatory, No. 80, Nandan Rd.,
Shanghai 200030, China
e-mail: junping.chen@shao.ac.cn

Y. Zhang
College of Surveying and Geo-Informatics, Tongji University,
No. 1239, Siping Rd., Shanghai 200092, China

J. Chen
School of Astronomy and Space Science,
University of Chinese Academy of Sciences, Beijing 100049, China

J. Sun et al. (eds.), *China Satellite Navigation Conference (CSNC) 2017 Proceedings: Volume II*, Lecture Notes in Electrical Engineering 438,
DOI 10.1007/978-981-10-4591-2_22

1 Introduction

In the BeiDou Navigation Satellite System (BDS) broadcast messages, the orbit parameters is generated through orbit fitting processing using the precise orbits of ODTS (Orbit Determination and Time Synchronization) process [1–3], while the satellite clock parameter is generated based on the TWTT (Two-Way satellite Time Transfer) technique [1, 3, 4]. BDS's Legacy PNT service performance is 10 m (95%) in positioning precision, and 50 ns (95%) timing precision at in Asia-Pacific area [5].

To improve positioning accuracy and integrity, BDS integrates the wide area differential services together with the Legacy PNT system. Current differential corrections include the Equivalent Satellite Clock for the combined correction for satellite radial orbit and clock errors, and ionospheric grids for the ionospheric correction improvement for single-frequency users [6, 7]. The current differential corrections provide for authorized users only, and the positioning precision can be improved by 50% for dual-frequency user and 30% for single-frequency user, respectively [7]. The Equivalent Satellite Clock correction principally includes the mean radial component of orbits error in BDS monitoring area and the real-time satellite clock errors, thus it could not fully reflect the orbit errors in the Along-track and Cross-track directions and its differences maybe at decimeter level for users at boundary areas of BDS service region. To correct for this effect, the orbit corrections based on the combined the epoch-differenced carrier phase and pseudo-range is proposed [8]. However, these models do not actually take advantage of the high precision carrier phase, as pseudo-range may be seriously biased by multipath and channel biases. Under such strategies, the User Differential Range Error (UDRE) is at a level of sub-meter level, which will limit the applications of higher accuracy requirements.

Supporting user decimeter level positioning accuracy requirements, a new type of differential correction, namely the zone correction, is proposed in the upgrading BDS wide area differential service system [9]. The new zone correction is generated using the high precision carrier phase and corrects for the remaining common errors for specific zones. In this paper, we firstly review the definition and calculation of zone correction. Precise Point Positioning (PPP) models for single- and dual-frequency observations using the zone corrections are introduced. Performance of the zone-divided PPP is evaluated for single- and dual-frequency observations, and strategies in handling of tropospheric and ionospheric delays are discussed.

2 Zone Correction and Zone-Divided PPP

2.1 Zone Correction

Most current wide area augmentation system uses smoothed pseudo-ranges in the calculation of wide area differential message, which is rather reliable and efficient in

real-time processing. However, due to the relative large noise of pseudo-range observations and the impact of multipath errors, the accuracy of the calculated differential correction is around 0.5 m in terms of UDRE [7, 8], which limits the current performance at the level of few meters and could not meet the requirement of real-time high precision applications.

To further improve the accuracy of differential corrections, the concept of zone correction is proposed and implement in the new BDS wide area differential service system [9]. The core of the algorithm is that both the observation error of a satellite and the remaining atmosphere correction error for a specified regional are assumed largely to be the same and are grouped into a time varying correction. Applying the new concept, service areas of BDS are divided into several regions. The zone correction is super-posed on broadcast ephemeris, the Equivalent Satellite Clock and the orbit corrections. It is represented by the combined residuals of carrier phase observations, where the receiver clocks and partial ambiguity are included, and are combined through a comprehensive combination process of multi-stations. The steps of zone correction are as follows:

(1) Calculation of Ionospheric-Free carrier phase residuals for each station in one zone:

$$dL(i,t) = LC - \rho - \delta_{rec} + \delta^{sat} - \delta_{trop} - \delta_{rela} - \delta_{amb} - \delta_{ESC} - \delta_{orb} + \varepsilon \quad (1)$$

In Eq. (1), L is the phase residuals of frequency i at time t, ρ is the geometric distance between tracking station and satellite computed from broadcast ephemeris, δ_{rec} is the appropriate station clock, δ_{sat} is the satellite clock computed from broadcast ephemeris, δ_{trop} is the tropospheric delay, δ_{rela} is the correction of relatively, δ_{amb} is the appropriate satellite ambiguity through pseudo-range minus carrier phase, δ_{ESC} is the Equivalent Satellite Clock Correction, δ_{orb} is the orbit correction, ε contains the phase-windup corrections, solid tide correction, ocean tide correction and the observation noise. It should be pointed out that the satellite clock in broadcast ephemeris is based on B3 frequency and the satellite clocks differs between different frequencies [10, 11], and TGD correction should be corrected for observations of other frequency combination.

From Eq. (1) we can see that the residual of carrier phase contains the residual of station clock and partial ambiguity, together with observation noise, residual of satellite orbit error, satellite clock error and tropospheric model error.

(2) Calculation of epoch-differenced carrier phase residual for each station in one zone.

$$\Delta L(i,t,t-1) = \begin{cases} 0, & t = 1 \\ dt(i,t) - dt(i,t-1), & t > 1 \end{cases} \quad (2)$$

(3) Combination of zone correction

$$dL(t) = f(\Delta L(t, t-1)) + dL(t-1) \tag{3}$$

In Eq. (3), f means the combination function of comprehensive carrier phase correction. In most situations, f is the weighted average of each station. During the case of satellite disappearing, satellite arising, cycle slips or station clock jumps, the process of cycle slip repairing and clock jump repairing should be performed, otherwise the data should be abandoned.

2.2 Model of Zone-Divided PPP

Based on the broadcast ephemeris, the Equivalent Satellite Clock, the orbit correction and precise phase zone correction, real-time PPP can be realized for both dual-frequency and single frequency users.

(1) Dual-frequency user PPP

For B1B2 or B1B3 frequency user, the positioning model can be expressed as follow by using ionospheric-free combination.

$$\begin{cases} PC = \rho + \delta_{rec} - \delta^{sat} + \delta_{trop} + \delta_{rela} + \delta_{ESC} + \delta_{orb} + \varepsilon_{PC} \\ LC = \rho + \delta_{rec} - \delta^{sat} + \delta_{trop} + \delta_{rela} + \delta_{amb} + \delta_{ESC} + \delta_{orb} + dL + \varepsilon_{LC} \end{cases} \tag{4}$$

In Eq. (4), PC and LC are the ionospheric-free pseudo-range and carrier phase combination of B1B2 or B1B3. Comparing Eq. (1) with Eq. (4), we can see that although the broadcast orbit and clock is not precise after Equivalent Satellite Clock correction and orbit correction, the residual error will be further corrected using the zone correction. The station clock residuals contains in the zone correction will absorbed by user station clock parameters, while the partial ambiguity in the zone correction will absorbed in user ambiguity parameter. The change of satellite orbit and clock remaining errors vary little during short time (90 or 180 s).

In the above model, the residuals mainly come from the carrier phase observation noise and the remained differences between station depended troposphere delay and the troposphere delay contained in zone correction. As for pseudo-range observations, the zone correction can't be used because the containment of partial ambiguity, so only the Equivalent Satellite Clock and orbit correction can be applied.

To study the impact of the troposphere delay difference on dual-frequency zone-divided PPP, tropospheric delay parameters could be theoretically set up in Eq. (4).

(2) Single frequency user PPP

For single frequency user, the ionosphere error is the main factor that affects the positioning precision. Currently, the BDS provide 8 parameter ionosphere model for legacy navigation, as for augmentation positioning, the 14 parameter ionosphere model or the ionosphere grids is used [10]. However, the correction precision is about 0.5 m [12, 13]. In 2002, GAO proposed a positioning model called UofC [14]. In this model, due to the opposite of ionospheric delay in pseudo-range and carrier phase, the ionospheric error can be eliminated by averaging pseudo-range and carrier phase. Based on UofC, we establish a single frequency zone-divided PPP model.

$$\begin{cases} P = \rho + \delta_{rec} - \delta^{sat} + \delta_{trop} + \delta_{\text{iono}} + \delta_{rela} + \delta_{ESC} + \delta_{orb} + \varepsilon_P \\ (P+L)/2 = \rho + \delta_{rec} - \delta^{sat} + \delta_{trop} + \delta_{rela} + \delta_{amb} + \delta_{ESC} + \delta_{orb} + dL + \varepsilon_L \end{cases} \tag{5}$$

In Eq. (5), P and L is the single frequency pseudo-range and carrier phase observation, $\delta_{iono}$is the ionospheric delay using 14 parameter ionosphere model or ionosphere grids. The other parameters are the same with Eq. (4). Which should be pointed out is that δ_{amb} is actually half of the carrier phase ambiguity at single frequency.

To study the impact of the ionosphere delay on single-frequency zone-divided PPP, phase observations corrected for ionospheric delay using 14 parameter ionosphere model or ionosphere grids could also be directly combined with pseudo-range observations in Eq. (5).

3 Data Processing Strategy

In the implementation of the zone correction for BDS wide area differential service system, the service area is divided into 18 zones, where the zone correction for each zone is assumed to be calculated based on a pseudo reference station at the center of the zone. Users first calculate its approximate coordinates and searching for the nearest zone according to the given table of coordinates of each zone center. The zone corrections are broadcasted to user through GEO satellite at given defined epoch. To evaluate the precision and reliability of zone correction, the zone-divided PPP performance is analyzed.

Figure 1 shows the region of each zone. About 30 BDS tracking stations distributed in China are selected for zone-divided PPP assessment, which are also showed in Fig. 1. For each station, the zone centers within 1000 km are selected orderly. The mean distance for all stations and zone centers is 597 km. Table 1 gives the processing strategy of zone-divided PPP.

Data from DOY 346–348 in 2016 is chose. For each day, the data is divided into 4 parts every 6 hours. So there are 12 arcs processed in total. For each arc, the B1B2, B1B3, B1, B2, B3 zone-divided PPP are computed in kinematic mode.

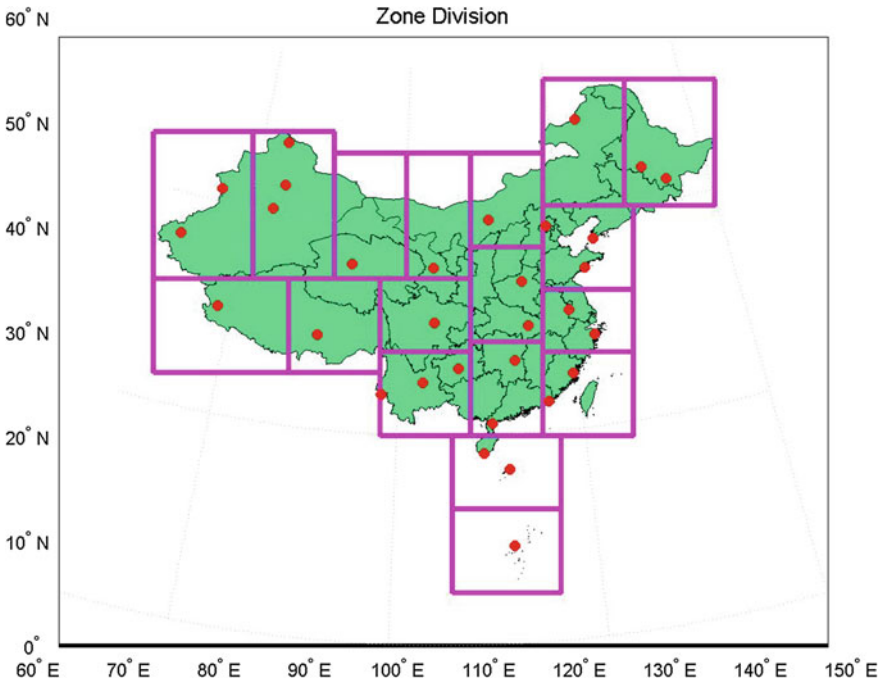

Fig. 1 Zone area and test stations

Table 1 Zone-divided PPP strategy

Type	Strategy
Estimator	Kalman filter
Satellite orbit and clock	Broadcast ephemeris
Augmentation message	ESC correction, orbit correction, zone correction
Data sampling	30 s
Limit elevation	10°
Ionospheric delay	Dual-frequency: Ionospheric-free combination; Single frequency: BDS ionosphere model
Tropospheric delay	GPT2w + SAAS + VMF1
Solid tide, ocean tide	IERS convention
Station coordinate	Estimated, white noise
Station clock	Estimated, white noise
Ambiguity	Estimated

4 Analysis of Zone-Divided PPP Performance

4.1 Effect of Troposphere Delay Parameter

Troposphere delay is one of the errors in GNSS observation. Troposphere models such as UNB3, EGNOS, GPT2, IGGtrop can estimate the hydrogen delay and most of wet delay, the precision of these models have been demonstrated to be 4–6 cm [15, 16]. The rest of the wet tropospheric delay is estimated as a random walk parameter in traditional PPP. As mentioned above, the zone correction contains tropospheric model error. After applying zone correction, the troposphere error would well be eliminated in areas near zone center.

To verify this, we make a comparison of zone-divided PPP with and without troposphere parameter estimation. The troposphere model of GPT2w is set as the initial value. Figure 2 shows the comparison of horizontal and vertical RMS distribution for B1B2 combined zone-divided PPP and Table 2 gives the statistical RMS of different data length. From the figures we can see that by fixing the troposphere delay, the precision of zone-divided PPP in height gets better. After fixing the troposphere delay, 87% of PPP result is better than 0.2 m in horizontal and 83% is better than 0.6 m in vertical for dual-frequency user. We can also find that there is no much difference on the precision during 2–4 and 4–6 h, which means the positioning error is already convergence (Table 2).

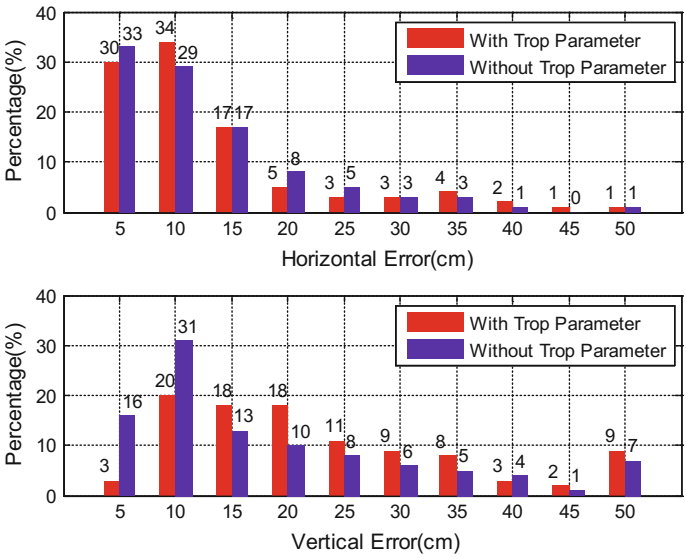

Fig. 2 Zone-divided PPP precision distributions at horizontal (*up*) and vertical (*down*) with and without troposphere parameter estimation

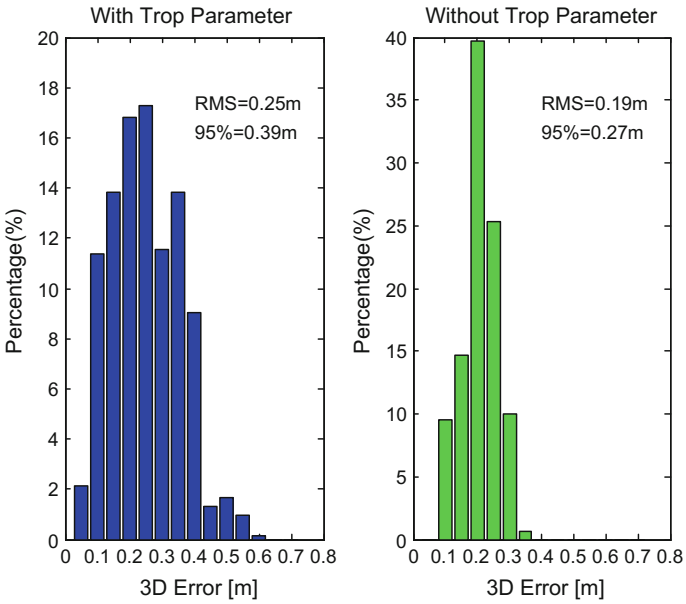

Fig. 3 Positioning error distribution of zone-divided PPP for B1B2 with and without troposphere parameter

Table 2 RMS of zone-divided PPP results at different data length

Type (h)	With troposphere parameter		Without troposphere parameter	
	Horizontal (m)	Vertical (m)	Horizontal (m)	Vertical (m)
1–2	0.17	0.28	0.17	0.24
2–4	0.11	0.22	0.11	0.18
4–6	0.10	0.22	0.10	0.17

To take a specific observation of positioning error distribution, the 3D positioning error distribution of zone-divided PPP at one station is compared by histogram statistics after one hour of convergence, showed in Fig. 3. The station is about 700 km away from the zone center. From the figure we can see that the 3D positioning RMS is 0.24 m and 95% is better than 0.39 m when estimating the troposphere parameter. While the 3D positioning RMS is 0.1 m and 95% is better than 0.27 m by fixing it. This proves that the zone correction contains part of tropospheric model error at a regional area.

4.2 *Effect of Single Frequency PPP Model*

As for single frequency user, one can use the traditional single frequency PPP model or the UofC model mentioned above. To evaluate the different of these two models, a comparison test is conducted. Figure 4 is a typical zone-divided PPP results for B1 frequency user of two models. From the figure we can see that the traditional model is much worse than UofC, which is due to that the ionosphere error is eliminated in UofC model by averaging pseudo-range and carrier phase.

To further evaluate the effect of zone correction on single frequency PPP, we also test the traditional single frequency PPP without zone correction. The statistical results for all stations are listed in Table 3. From the table we can see the advantage of UofC model. The RMS is 0.22 m in horizontal and 0.43 m in vertical. As for traditional PPP, the positioning precision also improves after applying zone correction, from 0.67/0.99 in horizontal and vertical to 0.42/0.87. To take a specific observation, the 3D positioning error distribution at one station is compared in Fig. 5. After applying zone correction, the 3D positioning RMS improves from 1.38 to 1.04 m, as for 95% positioning error, it improves from 2.03 to 1.59 m.

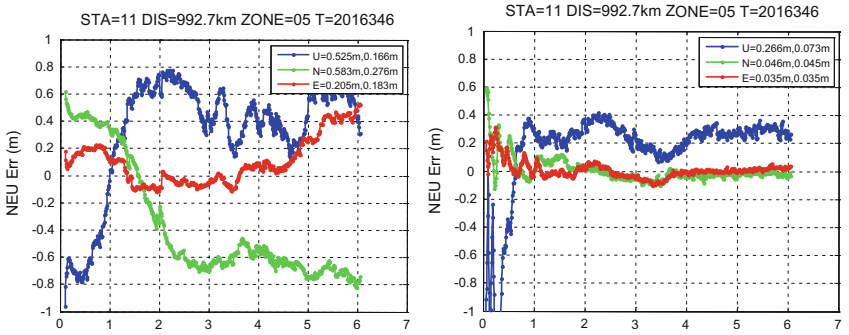

Fig. 4 Traditional single frequency PPP (*left*) versus UofC PPP (*right*)

Table 3 Single-frequency PPP for different model

Type	Traditional PPP without zone correction	Traditional PPP with zone correction	UofC PPP with zone correction
Horizontal (m)	0.67	0.42	0.22
Vertical (m)	0.99	0.87	0.43

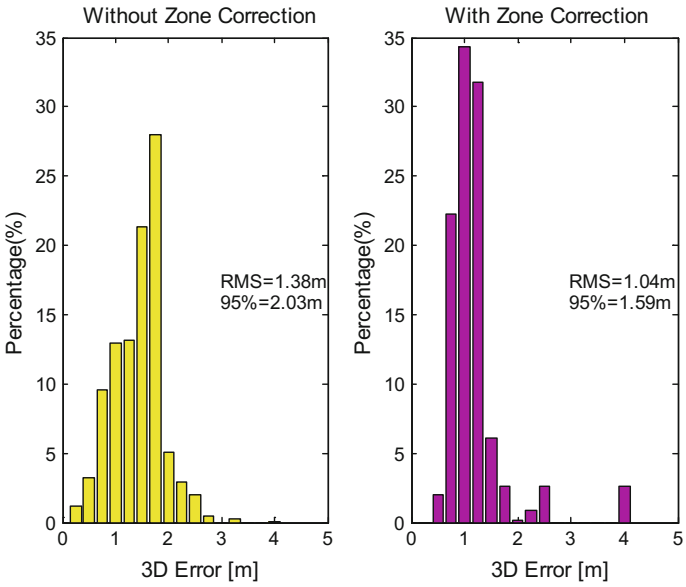

Fig. 5 Positioning error distribution of zone-divided PPP for B1 with and without zone correction

4.3 Overview of Zone-Divided PPP Performance

Based on the analysis of effect of troposphere delay parameter and single frequency PPP model analyzed above. We conduct the full experiment of zone-divided PPP for different frequencies. In the experiment, the troposphere error is fixed through GPT2w model. For single frequency positioning, the UofC model is applied. The RMS of zone-divided PPP is calculated from 4th to 6th hour. Table 4 gives the mean value of all stations and zones of different frequencies. We can see that for dual-frequency user, the mean kinematic positioning precision is below 0.15 m in horizontal and 0.20 m in vertical. As for single frequency user, the mean kinematic positioning precision is below 0.30 m in horizontal and 0.50 m in vertical, respectively. The single frequency zone-divided PPP performance is much worse than that of dual-frequency. The precision can be regarded as the zone-divided precision within 600 km.

For real-time kinematic user, the convergence performance is more concerned. To evaluate the convergence performance of all stations, we get the mean 3D positioning error of zone-divided PPP every 5 min at first one hour. Figure 6 gives

Table 4 RMS of zone-divided PPP results at different frequencies

	B1B2	B1B3	B1	B2	B3
Horizontal (m)	0.11	0.14	0.22	0.23	0.27
Vertical (m)	0.18	0.19	0.43	0.43	0.46

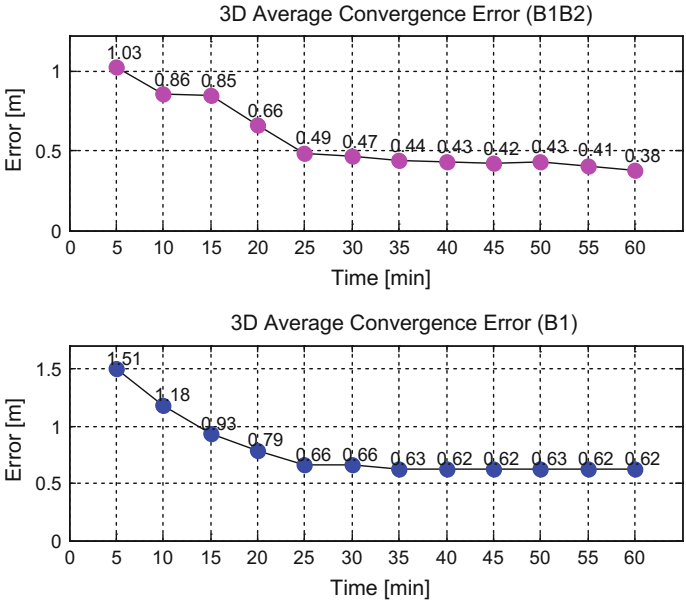

Fig. 6 Convergence statistics of zone-divided PPP for B1B2 (*up*) and B1 (*down*)

the convergence performance of zone-divided PPP for B1B2 and B1. From the figure we can see that it can convergence to 0.5 m in 25 min for dual-frequency user and to 0.8 m in 20 min for single frequency user.

5 Conclusions

In this paper we give a brief introduction of zone correction and the zone-divided PPP model for dual- and single-frequency user. Based on national distributed BDS tracking station in mainland China we evaluate the performance of dual- and single-frequency zone-divided PPP in different aspects. We conclude that:

(1) The precision of zone-divided PPP improves after fixing the troposphere delay.
(2) Zone correction improve the user positioning performance. UofC model is much better for single frequency user.
(3) For dual-frequency user, the mean kinematic positioning precision is below 0.15 m in horizontal and 0.20 m in vertical. As for single frequency user, the mean kinematic positioning precision is below 0.30 m in horizontal and 0.50 m in vertical, respectively.
(4) The zone-divided kinematic PPP can convergence to 0.5 m in 25 min for dual-frequency user and to 0.8 m in 20 min for single frequency user within 600 km. In general, the user can achieve a positioning precision better than 1 m within the distance of 1000 km from zone center.

Acknowledgement This work is support by 863 project (2014AA123102) and NSFC 11673050 and 11273046.

References

1. Zhou SS, Hu XG, Wu B et al (2011) Orbit determination and time synchronization for a GEO/IGSO satellite navigation constellation with regional tracking network. Sci China Phys Mech Astron 54:1089–1097
2. Zhou SS, Cao YL, Zhou JH et al (2012) Positioning accuracy assessment for the 4GEO/5IGSO/2MEO constellation of COMPASS. Sci China Phys Mech Astron 55:2290–2299
3. Tang CP, Hu XG, Zhou SS et al (2016) Improvement of orbit determination accuracy for BeiDou Navigation Satellite System with two-way satellite time frequency transfer. Adv Space Res 58(7):1390–1400
4. He F, Zhou SS, Hu XG et al (2014) Satellite-station time synchronization information based real-time orbit error monitoring and correction of navigation satellite in BeiDou System. Sci China Phys Mech Astron 57:1395–1403
5. Yang Y, Li J, Xu J et al (2011) Contribution of the compass satellite navigation system to global PNT users. Sci Bull 56(26):2813–2819
6. Wu XL, Zhou JH, Wang G et al (2012) Multipath error detection and correction for GEO/IGSO satellites. Sci China Phys Mech Astron 55:1297F02D1306, doi:10.1007/s11433-012-4741-6
7. Cao YL, Hu XG, Wu B et al (2012) The wide-area difference system for the regional satellite navigation system of COMPASS. Sci China Phys Mech Astron 55:1307–1315
8. Chen J, Yang S, Zhou J (In Press) A new pseudo-range/phase combined SBAS differential correction model. Acta Geod Cartogr Sin
9. Chen J, Zhang Y, Yang S, Wang J (2015) A new approach for satellite based GNSS augmentation system: from sub-meter to better than 0.2 meter era. In: Proceedings of the ION 2015 Pacific PNT meeting, pp 180–184
10. China Satellite Navigation Office (2013) BeiDou Navigation Satellite System signal in space interface control document open service signal (Version 2.0), 2013.12
11. Li H, Zhu W (2014) Inter frequency clock bias of BeiDou. Acta Geod Cartogr Sin 43 (11):1127–1131
12. Wu XL, Hu XG, Wang G et al (2013) Evaluation of COMPASS ionospheric model in GNSS positioning. Adv Space Res 51(6):959–968
13. Wu XL, Zhou JH, Tang B et al (2014) Evaluation of COMPASS ionospheric grid. GPS Solut 18(4):639–649
14. Gao Y, Shen X (2002) A new method of carrier phase based precise point positioning. J Navig 49(2):109–116
15. Bohm J, Moller G, Schindelegger M (2014) Development of an improved empirical model for slant delays in the troposphere (GPT2w). GPS Solut
16. Li W, Yuan YB, Ou JK et al (2012) A new global zenith tropospheric delay model IGGtrop for GNSS applications. China Sci Bull 57:2132–2139. doi:10.1007/s11434-012-5010-9